

Directivity of near-fault ground motion generated by thrust-fault earthquake: a case study of the 1999 M_w7.6 Chi-Chi earthquake

J.J. Hu¹ and L.L. Xie²

¹Assistant Professor, Dept. of Engineering Seismology and Strong Motion Observation, IEM, Harbin, China

²Professor, Dept. of Engineering Seismology and Strong Motion Observation, IEM, Harbin, China

Email: hu-jinjun@163.com, hujinjun@iem.net.cn

ABSTRACT :

Characteristics of near-fault ground motion resulting from different fault mechanisms were considered the dominant factor in developing input ground motion for structures in near-fault region. Interpretations of near-fault ground motions from 139 free-field stations of 1999 Chi-Chi earthquake show that, except for the hanging-wall and footwall effect generated by the dipping-fault geometry, directivity effect is also an important factor in considering the near-fault ground motions, which may largely affect the distribution and intensity of ground motion in near fault region. Based on the selected hard site ground motions, the peak ground acceleration, response spectra and time histories were investigated respectively. Results show that for similar site condition in the opposite directions of fault rupture (forward and backward), the characteristics of three components of ground motion, including fault-normal, fault-parallel and vertical, can varies significantly, mainly because of the constructive interference of radiated seismic energy, as the Chelungpu fault translated into predominantly left-lateral rupture in the north part.

KEYWORDS: Near-fault ground motion; Thrust-fault earthquake; Directivity effect; Hanging-wall effect

1. CHI-CHI EARTHQUAKE

The 1999 M_w7.6 Chi-Chi earthquake was the largest thrust earthquake occurred in Taiwan in the twentieth century (Ma *et al.*, 2001). The strong shaking caused long surface rupture, heavy building damage and human casualties. At the same time, it produced quantities of valuable near-fault strong ground motions with high quality and abundant engineering damage materials for studying new attenuation relationship, source process, site effect, hanging wall/foot wall effect and etc. Many studies has concentrated on the characteristics of near-fault ground motions of this thrust earthquake(Chang *et al.*, 2001, 2004; Aagaard *et al.*, 2004; Boore, 2001a; Chen *et al.*, 2001; Dalguer *et al.*, 2001; Fletcher and Wen, 2005; Lee *et al.*, 2001; Loh *et al.*, 2001; Ouchi *et al.*, 2001; Shin and Teng, 2001; Sokolov *et al.*, 2002; Wang *et al.*, 2001, 2003, 2004; Wen *et al.*, 2001; Wu *et al.*, 2001). And also, based on the abundant high quality seismic data, the kinematical and dynamical source process of the Chi-Chi earthquake had been carried out by many literatures (Chung and Shin, 1999; Ma *et al.*, 2001; Oglesby and Day, 2001; C. Wu *et al.*, 2001; Lin, 2001; Zeng and Chen, 2001; Wang *et al.*, 2001; Yoshioka, 2001; Dalguer *et al.*, 2001).

1.1. Finite source model

The M_w 7.6 Chi-Chi earthquake occurred on a north-south trending fault in western Taiwan, with a extensive surface rupture of about 80 km(Oglesby and Day, 2001; Chin *et al.*, 2000). Inversions of source process show that Chi-Chi earthquake took place on a complex thrust fault, with dip angle of about 30° to the east, and at the end part of Chelungpu fault the rupture turns into mainly oblique-slip movement (Ma *et al.*, 2000, 2001; Chi *et al.*, 2002; Sekiguchi *et al.*, 2002; Johnsson *et al.*, 2002; Wu *et al.*, 2002; Zeng and Chen, 2002). Table 1 provides some source parameters of finite fault model. Figure.1 shows the fault geometry and finite fault model of Chi-Chi earthquake (Ma *et al.*, 2001).

Table. 1 Source parameters of Chi-Chi earthquake

	Depth (km)	M _w	M ₀ (Nm)	Strike (deg)	Dip (deg)	Rake (deg)	Length (km)	Width (km)	Rupture speed (km/s)
Ma <i>et al.</i> , (2001)	7.00	7.69	3.87e+20	5.0	30.0	55.0	105	40	2.5
Chi <i>et al.</i> , (2002)	8.00	7.68	3.73e+20	5.0	30.0	55.0	112	45.5	2.6
Sekiguchi <i>et al.</i> , (2002)	7.00	7.63	3.11e+20	5.0	30.0	55.0	78	39	2
Johnsson <i>et al.</i> , (2002)	8.80	7.58	2.66e+20	5.0	23.0	55.0	104	30	-
Wu <i>et al.</i> , (2002)	6.90	7.67	3.59e+20	5.0	30.0	55.0	85	49	3
Zeng and Chen, (2002)	6.80	7.61	2.91e+20	5.0	27.5	55.0	84	42	2.5

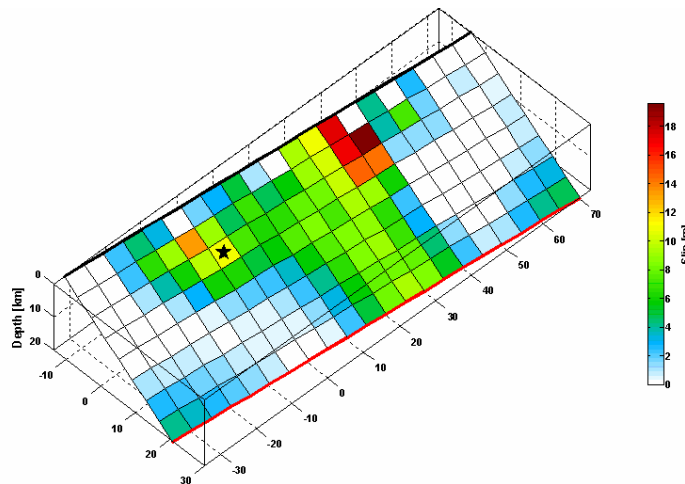


Figure. 1 Fault geometry and finite fault model of Chi-Chi earthquake (Ma *et al.*, 2001)

1.2. Strong Ground motion selection

The ground motion data were obtained from the PEER Strong Motion Database. In order to isolate the site effect, we select 139 hard site recordings from the totally 297 stations. Site classification method is adopted from the Central Weather Bureau. Figure.2 shows the hard site, medium site and soft site categories, as well as, the surface rupture of Chelungpu fault. According to the orientation and the location to the fault trace of each station, all the near-fault stations are divided into four groups: forward direction stations, backward direction stations, hanging wall side stations and foot wall side stations, and each kind of station is represented by triangle, circle, diamond and star, respectively, in Figure 3. According to the fault geometry and finite fault model (Figure 1), Forward direction (FD) stations are those stations located beyond the end of the rupture, backward direction (BD) stations are located in front of the initiation of the rupture, hanging wall (HW) side stations are located on the hanging wall and foot wall (FW) side stations are located on the foot wall side of the dip fault.

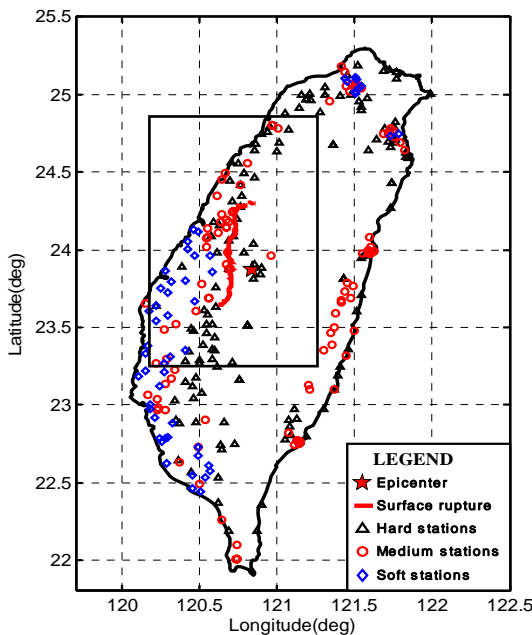


Figure. 2 PEER stations and surface rupture of Chi-Chi earthquake

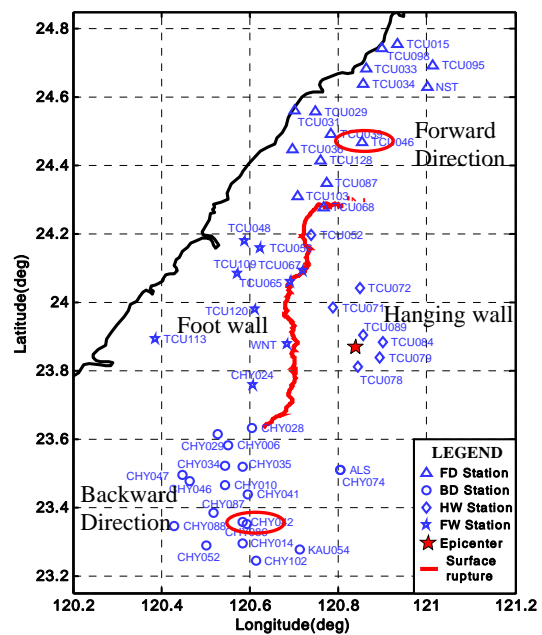


Figure. 3 Selected near-fault hard site stations of Chi-Chi earthquake

2. ROTATION OF GROUND MOTION

The original acceleration recordings of horizontal components are NS and EW oriented. For the purpose of investigating the effect of directivity on different component, we rotate the original orientations of horizontal components into Fault-Normal (FN) and Fault-Parallel (FP) components. Figure 4 shows the method of rotating arbitrary couple of orthogonal components into FN and FP components. Equation (2.3) gives the relation between the original and rotated components. Where H_{Old}^1 and H_{Old}^2 represent the amplitude at a given time of the two horizontal components, respectively, and α_{Old} represents the original azimuth of the first component in clockwise. Thus, the rotated FN and FP components are represented by H_{Old}^1 and H_{Old}^2 , respectively, with the azimuth α_{new} of the rotated first component in clockwise. Note that the above method are conducted on the premise that each point on the two horizontal components occurs simultaneously (Personal Communication, Evans, 2007).

We define β as the angle needed to rotate

$$\beta = \alpha_{Old} - \alpha_{New} \quad (2.1)$$

Then we get a Rotation Matrix (RM)

$$\text{RM} = \begin{pmatrix} \cos(\beta) & \sin(\beta) \\ -\sin(\beta) & \cos(\beta) \end{pmatrix} \quad (2.2)$$

According to Figure 4, the rotated ground motion vector is

$$\begin{pmatrix} H_{New}^1 \\ H_{New}^2 \end{pmatrix} = \text{RM} * \begin{pmatrix} H_{Old}^1 \\ H_{Old}^2 \end{pmatrix} \quad (2.3)$$

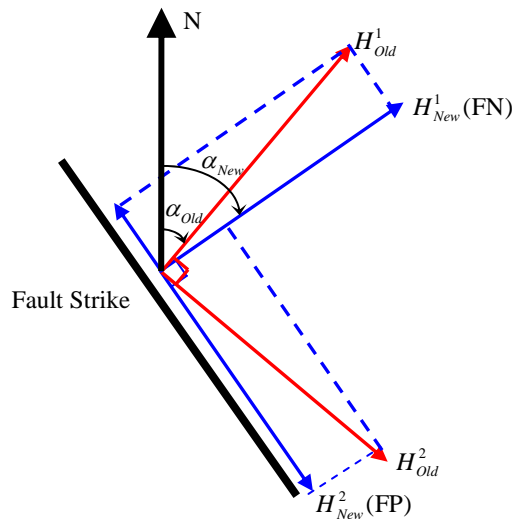


Figure. 4 Rotation of horizontal components to FN and FP components

To investigate the directivity effect on near-fault ground motion of Chi-Chi earthquake, three aspects are considered, including amplitude distribution, response spectra and time history. Below gives the detailed analysis of each aspect.

3. PGA COUNTER MAPS

In order to investigate the characteristics of amplitude distribution, based on the rotated 139 hard site ground motions, we take advantage of the peak ground acceleration (PGA) of each station, and draw it on the sketch map of Taiwan. Figure 5 shows the contour maps of PGA of the two horizontal (FN, FP) and vertical component. Read line denotes the rupture trace of Chelungpu fault, read star denotes the epicenter and triangles denote the hard site stations.

It is obvious that there exists a strong hanging wall and foot wall effect on the PGA and its decreasing tendency between the two sides of the fault trace (Chang *et al.*, 2004), and which was caused by the source mechanism of a thrust fault earthquake (Abrahamson and Somerville, 1996; Oglesby *et al.*, 1998, 2000a, 2000b). Whereas, is there any directivity effect on ground motion in the forward direction and backward direction? To answer this question we look into two aspects, one is the amplitude or PGA, another is the decreasing tendency of the amplitude. On the one hand, from the below three components we can see that, on the whole, the peak ground motion in the rupture end of the fault is a little bigger than that of the beginning part. On the other hand and more importantly, the effect of directivity on the PGA's decreasing tendency is much clearer than that on the amplitude. Specifically, the PGA decreases fast at the beginning part of the fault while it decreases slowly at the end part of the fault, this phenomenon can be seen in any of the three components (see Figure 5).

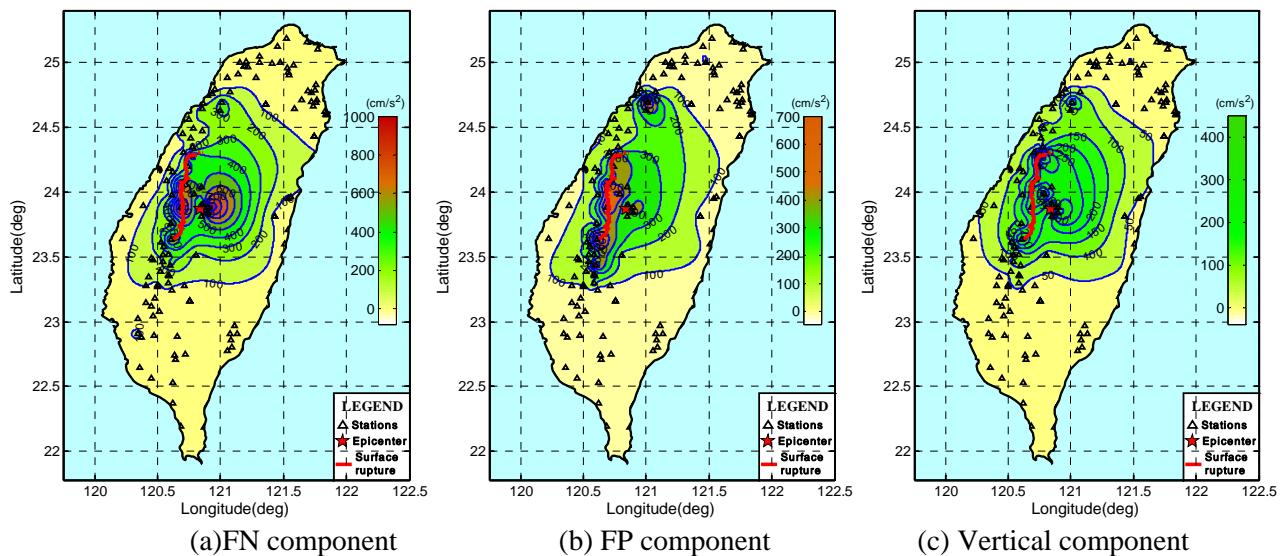


Figure. 5 PGA contour maps of hard site stations.

4. COMPARISON OF RESPONSE SPECTRUM

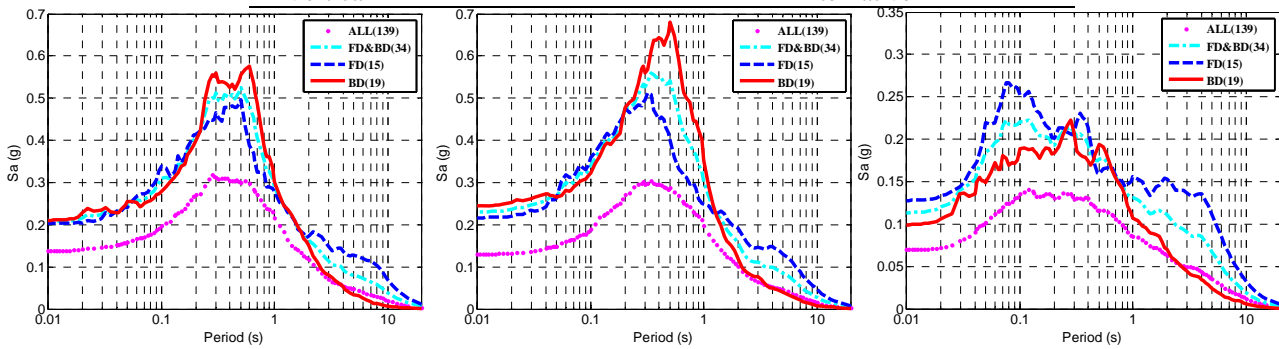
In this section, the effect of directivity on the spectral content of ground motions is analyzed. To show the difference between the forward and back ward direction, the acceleration response spectrum of 5% damping ratio are adopted. As shown in Figure 3, the selected 50 near-fault stations are divided into four districts, FD, BD, HW and FW. In order to isolate the effect of the hanging wall and foot wall on the ground motion of FD BD stations as much as possible, only those response spectrum which are located within the two opposite directions are compared. Figure 6 gives the average response spectrum of ground motions in FD and BD. Where, the blue dash line represents the average spectra of the 15 FD stations, while the red solid line represents the average spectra of the 19 BD stations. We also give the average spectra of all the 139 hard site stations, and which is denoted by the pink dot line in Figure 6.

Through comparing the average response spectra of the FD and BD stations we find that, for the FN component as can be seen in Figure 6 (a), in short period of 0.2s -1.0s, the amplitude of response spectra in BD is larger than that in FD. Whereas, for periods larger than 2s, the spectral amplitude gets larger in FD than that in BD. For the FP component shown in Figure 6 (b), there is a similar tendency with the FN component aspect in the comparison of FD and BD response spectrum. In detail, the amplitude of response spectra in BD is larger than that in FD in short period of 0.2s -1.1s. And for periods larger than 1.1s, the spectral amplitude gets larger

in FD than that in BD. As for the vertical component which is shown in Figure 6 (c), there is some difference compared with the horizontal components. Except for periods within 0.2s-0.8s that the spectral amplitudes of FD and BD alternate up and down along the transverse axis, the spectral amplitude of FD is greater than that of BD in all the other periods. Table 2 provides the detailed description of spectral amplitude in FD and BD of the three components.

Table 2 Comparison of spectral amplitude in FD and BD

Component	Periods (T)			
	$T < 0.05s$	$0.05s \leq T < 0.2s$	$0.2s \leq T < 1.0s$	$T \geq 1.0s$
FN	FD \leq BD	FD $>$ BD	FD $<$ BD	FD \geq BD
FP	FD $<$ BD	FD $>$ BD	FD $<$ BD	FD \geq BD
Vertical	FD $>$ BD	FD $>$ BD	Alternative	FD $>$ BD



(a)FN component (b) FP component (c) Vertical component

Figure. 6 Comparison of response spectrum of FD and BD stations.

5. COMPARISON OF TIME HISTORIES

The acceleration time histories in FD and BD also bear the effect of directivity. In this section we choose two typical stations located in the two opposite directions with similar distance to the fault edge, one is TCU046 in FD and another is CHY042 in BD, which are marked by red ellipses in Figure 3. As usual, the original NS and EW components are rotated into FN and FP components, and then we compared the FD and BD seismograms within the same direction (see Figure 7, the upper is in FD and the lower is in BD).

Results indicate that ground motions in BD have a relatively longer engineering duration than that in FD. In other words, the energy is distributed in a relatively longer time in BD than that in FD. Thus, although the amplitude of ground motion in BD is smaller than that in FD, it's has a longer duration in BD than in FD. Further more, this makes it important to take into account the duration factor for the seismic design of structures located near the backward directions.

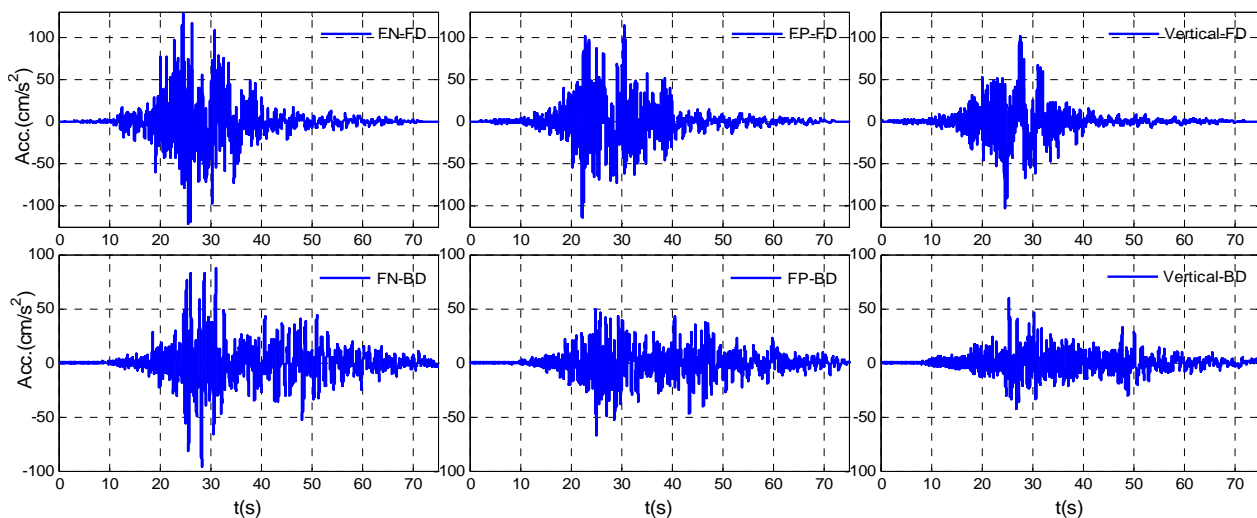


Figure 7 Comparison of ground motion in FD and BD

6. CONCLUSIONS

Although it is difficult to quantify directivity effect accurately because of the complexity of near-fault ground motion due to the uncertainty of source process, path effect and site conditions. Still, some conclusions based on the selected hard site ground motions can be drawn.

- 1) The PGA value and its decreasing tendency is affected by the rupture directivity. On the whole, amplitude in FD is a little bigger than that in BD, and more importantly, the amplitude decreases faster in BD than that in FD.
- 2) Effect of directivity on response spectra of ground motion is related to the period or frequency. In general, the spectral amplitude in long period are much more easier to be affected by the directivity effect, and the spectral amplitude in FD is thought to have a large value than that in BD.
- 3) The time history of ground motion in BD contains a relatively longer engineering duration compared with that in BD.

REFERENCES

- Aagaard, B. T. Hall, J. F. and Heaton, T. H. (2004). Effects of Fault Dip and Slip Rake Angles on Near-Source Ground Motions: Why Rupture Directivity Was Minimal in the 1999 Chi-Chi, Taiwan, Earthquake. *Bull. Seism. Soc. Am.*, 94(1): 155 - 170.
- Abrahamson, N. A. and Somerville, P. G. (1993). Estimation of hanging wall and foot wall effects on peak acceleration, Proc. International Workshop on Strong Motion Data, Menlo Park, California, Vol. II, 351-360.
- Chang, T. Y., Cotton, F., Tsai, Y. B. and Angelier, J. (2004). Quantification of hanging-wall effects on ground motion: Some insights from the 1999 Chi-Chi earthquake. *Bull. Seism. Soc. Am.*, 94 (6): 2186-2197.
- Fletcher, J. B. and Wen, K. L. (2005). Strong Ground Motion in the Taipei Basin from the 1999 Chi-Chi, Taiwan, Earthquake. *Bull. Seism. Soc. Am.*, 95(4): 1428 - 1446.
- Lee, W. H. K., Shin, T. C., Kuo, K. W., Chen, K. C. and Wu, C. F. (2001). CWB Free-Field Strong-Motion Data from the 21 September Chi-Chi, Taiwan, Earthquake. *Bull. Seism. Soc. Am.*, 91(5):1370 - 1376.
- Oglesby, D. D. and Day, S. M. (2001). Fault Geometry and the Dynamics of the 1999 Chi-Chi (Taiwan) Earthquake. *Bull. Seism. Soc. Am.*, 91(5): 1099-1111.
- Oglesby, D. D., R. J. Archuleta, and S. B. Nielsen (2000a). The dynamics of dip-slip faults: explorations in two dimensions, *J. Geophys. Res.* 105,13,643 -13,653.
- Oglesby, D. D., R. J. Archuleta, and S. B. Nielsen (2000b). The three-dimensional dynamics of dipping faults, *Bull. Seism. Soc. Am.* 90,616 -628.
- Ouchi, T., Lin, A., Chen, A. and Maruyam, T. (2001). The 1999 Chi-Chi (Taiwan) Earthquake: Earthquake Fault and Strong Motions. *Bull. Seism. Soc. Am.*, 91(5): 966 - 976.
- Shin, T. C. and Teng, T. L. (2001). An Overview of the 1999 Chi-Chi, Taiwan, Earthquake. *Bull. Seism. Soc. Am.*, 91(5): 895 - 913.
- Somerville, P. G. and Smith, N. F. (1996). "Forward rupture directivity in the Kobe and Northridge earthquakes, and implications for structural engineering." *Seismological Research Letters*, 67(2), pp. 55.
- Somerville, P. G., N. F. Smith, R. W. Graves, and N. A. Abrahamson (1997). "Modification of empirical strong ground motion attenuation relations to include the amplitude
- Somerville, P., C. K. Saikia, D. Wald, and R. Graves (1995). "Implications of the Northridge
- Somerville, P., K. Irikura, R. Graves, S. Sawada, D. Wald, N. Abrahamson, Y. Iwasaki, T. Kagawa, N. Smith, and A. Kowada (1999) . Characterizing crustal earthquake slip models for the prediction of strong ground motion, *Seism. Res. Lett.*, 70, 59-80, 1999.
- Phung, V., Atkinson, G. M. And Lau, D. T. Characterization of directivity effects observed during 1999 chi-chi, taiwan earthquake. 13th World Conference on Earthquake Engineering, Vancouver, B.C., Canada, August 1-6, 2004, Paper No. 2740
- Teng, T. L., Tsai, Y. B. and Lee, W. H. K. (2001). Preface to the 1999 Chi-Chi, Taiwan, Earthquake Dedicated Issue. *Bull. Seism. Soc. Am.*, 91(5): 893 - 894.
- Wang, G. Q., Zhou, X. Y., Ma, Z. J. and Zhang, P. Z. (2001). A Preliminary Study on the Randomness of Response Spectra of the 1999 Chi-Chi, Taiwan, Earthquake. *Bull. Seism. Soc. Am.*, 91(5):1358 - 1369.
- Wen, K. L., Peng, H. Y., Tsai, Y. B. and Chen, K. C. (2001). Why 1G Was Recorded at TCU129 Site During the 1999 Chi-Chi, Taiwan, Earthquake. *Bull. Seism. Soc. Am.*, 91(5): 1255 - 1266.